Scenario Analysis of Earthquake Risk in Thimphu

Final Report prepared for Geohazards International

February 2023

Verisk™

Contents

Acknowldegements

The Verisk and GeoHazards International would like to thank the members of the Thimphu Earthquake Hazard Working Group for their guidance, advice, and expertise; and for reviewing the earthquake scenarios and reports. We are grateful for the support from the Royal Government of Bhutan's Department of Disaster Management, without whom the project would not have been possible. We also wish to thank each of the government and non-government officials who participated in the final workshop to take the results forward.

Thimphu Earthquake Hazard Working Group Members

- Dr. Dowchu Dukpa, Chief Seismologist, Department of Geology and Mines
- Mr. Karma Namgay, Geologist, Department of Geology and Mines
- Mr. Sangay Rinzin, GIS officer, Department of Human Settlement
- Mr. Jigme Wangdi, Engineer, Department of Engineering Services
- Mr. Yeshi Wangdi, Executive Engineer, Thimphu Thromde
- Mr. Sonam Tshewang, Executive Engineer, Department of Disaster Management

Participants in the Stakeholders Workshop on Increasing Building Resilience to Earthquake Damage, 26th July 2022, Thimphu Bhutan

- Thinley Wangchuk, Hydrology/Meteorology Officer, National Center for Hydrology and Meteorology
- Sonam Choki, Hydrology/Meteorology Officer, National Center for Hydrology and Meteorology
- Jigme Wangdi, Deputy Executive Engineer, Department of Engineering Services
- Nityam Nepal, Senior Geologist, Department of Geology and Mines
- Tshewang Nidup, Lecturer, College of Science and Technology
- Nimesh Chhetri, Associate Lecturer, College of Science and Technology
- Nima Lhamu, Engineer, Construction Development Board
- Hem Bdr. Bhattarai, GIS officer, Department of Human Settlement
- Chenzom, Principal Engineer, Bhutan Standard Bureau
- Cheki Zangmo, Engineer, Bhutan Standard Bureau
- Karma Tshetrim, Chief Engineer, Bhutan Standard Bureau
- Pema, Executive Engineer, Department of Culture
- Chendra Norbu, Assistant Programme Officer, School Planning & Coordination Division
- Tshering Wangdi, Engineer, Royal Insurance Corporation of Bhutan
- Kuenzang Nima, Assistant Programme Officer, Emergency Medical Services Division
- Tshering Zam, Assistant Manager, Bhutan Insurance Limited
- Dorji Yangzom, Development Officer, Bhutan Insurance Limited

- Jangchub Peldon, Civil Engineer, National Housing Development Corporation
- Passang Dorji Moktan, Civil Engineer, National Housing Development Corporation
- Sonam Tshewang, Executive Engineer, Department of Disaster Management
- Tsutomu Sakakiyama, Senior Volunteer, Department of Disaster Management

GeoHazards International (GHI) contributors

- Mr. Yeshey Lotay, National Coordinator, GHI Bhutan Office
- Ms. Heidi Stenner, Project Manager
- Veronica Cedillos, President and CEO
- Hari Kumar, Regional Coordinator

Verisk Contributors

- Dr. Luis Souza, Senior Lead, Research and Resilience
- Mr. John Schneyer, Risk Consultant, Global Resilience Practice
- Mr. Daniel Raizman, Manager, Global Resilience Practice
- Ms. Erika Anderson, Risk Analyst, Global Resilience Practice
- Dr. Roger Grenier, Senior Vice President, Global Resilience Practice Lead

Executive Summary

This report summarizes the results of a scenario-based seismic risk analysis for the City of Thimphu, Bhutan conducted by Verisk (formerly AIR Worldwide) in collaboration with GeoHazards International (GHI). The project was conducted on behalf of the Department of Disaster Management, Royal Government of Bhutan (RGoB) to improve understanding of building vulnerability and to quantify the potential property damage from large earthquake events. The results will assist RGoB efforts in educating citizens, improving disaster preparedness, and enhancing building practices to minimize damage and loss of life.

The study was conducted in three phases 1) Review of Hazard, Exposure and Vulnerability; 2) Thimphu building inventory; and 3) Model Implementation and Results. Details for the first phase of study were provided in an Interim Report issued to GHI in February 2020. The results of phase 1 are summarized, along with additional commentary. This report focuses on the results of phases 2 and 3.

An existing earthquake model developed by the Global Earthquake Model Foundation (GEM) was incorporated into the Verisk modeling platform to compute losses from two earthquake scenarios: a regional magnitude (Mw) 8 event on the Main Himalayan Thrust (MHT) similar to the 1714 Earthquake, and a local Mw7 event along the Dhubri-Chunthang Fault Zone (DCFZ). Using a number of different ground motion prediction equations (GMPEs) for each scenario, 200 simulations were created in order to encompass the range of potential hazard.

The model study utilized a building inventory developed by GHI in collaboration with local officials in Thimphu. Verisk prepared the exposure data, generated hazard footprints and damage functions, and designed and executed sensitivity analyses aimed to assess the impact of different modeling assumptions. Additionally, this project also provided the opportunity to demonstrate Model Builder, Verisk's custom model development platform, a necessary tool to incorporate GEM's earthquake model and other localized third-party data, which was used for the analyses in this report.

The key findings from this analysis are as follows:

- Estimated losses are approximately $400m for the Mw8 scenario and $50m for the Mw7 scenario, with results sensitive to the choice of ground motion prediction equations (GMPEs).
- Modeled damage ratios for the two scenarios and the relative vulnerability by construction class align with estimates developed from the Verisk model for India, providing a reasonable benchmark for the GEM model implementation.
- Modeled losses and collapse probabilities for masonry buildings far exceed those estimated for reinforced concrete buildings

- Collapse probabilities are highly uncertain, with estimates provided here likely underestimates. Collapse estimates are subject to significant uncertainty.

Background and Project Motivation

The Kingdom of Bhutan is located on the eastern ridges of the Himalayas, in a region susceptible to large, damaging earthquakes. While the country is affected by additional natural hazards, including floods, landslides, wildfires and windstorms (Wangchuk, 2017), the high seismic hazard and vulnerability of the building stock combine to create significant risk of building damage and loss of life.

Recent studies detail the seismic risk in the country and the potential impacts of large damaging events (e.g., Stevens, et al, 2020, Hetényi, et al. 2016). Additional work by the World Bank and associated entities have also focused on risk to Thimphu, the capital city of Bhutan with a population of over 100,000 people. This study contributes to the growing body of work around earthquake risk in Bhutan by considering the impacts of two earthquake scenarios affecting the capital city.

In collaboration with GeoHazards International (GHI), Verisk conducted this study through a team from the Verisk company formerly known as AIR Worldwide (AIR). The motivation for this project was to aid the Royal Government of Bhutan (RGoB) in its effort to increase resiliency against seismic risk within the capital city of Thimphu. The aim is to provide the RGoB a quantification of building loss in Thimphu to inform ongoing work to identify and prioritize building safety, educate citizens, and strengthen disaster risk management. To this end, a primary goal of the effort was to engage local stakeholders, which was achieved by organizing the Thimphu Earthquake Hazard Working Group comprised of local government officials, scientific experts, and local and industry representatives formed by the Department of Disaster Management. Working Group members provided valuable expertise and directly contributed to the success of the project.

This report is organized as follows. First, a summary of the methodology is presented, drawing upon work previously described in the AIR interim report (AIR Worldwide, 2020). Next, we present a discussion of the exposure data, including the building survey and assumptions used in modeling. We then present the selected Mw7 and Mw 8 scenarios and detail the hazard and vulnerability components used in the model. The report concludes with presentation and discussion of the modeling results.

Methodology Overview

The following section describes an overview of the methodology followed to generate building loss from the earthquake scenarios in Thimphu. The technical details of the modeling effort are presented in AIR's interim report to GHI (AIR Worldwide, 2020), with additional commentary presented here and in the following sections of this report.

At the outset of the project, AIR reviewed a prior study of earthquake risk in Thimphu presented in an undated report by the World Bank. The report describes a hazard assessment for the city including assembly of a seismic risk catalog, discussion of ground motion prediction equations (GMPEs), and development of vulnerability functions. The work also included creation of a geographic information system (GIS) database of buildings in Thimphu, using information provided by municipal officials. The risk analysis was carried out using CAPRA, a disaster risk information platform.

While the World Bank study provided useful background, utilizing the model and exposure data and the CAPRA platform from the prior work proved challenging; for that reason and the fact the current modeling effort was focused on only two scenarios (not a full seismic risk assessment) the team chose to take a fresh approach, deploying an existing earthquake model developed by the Global Earthquake Model Foundation (GEM). Familiarity with the GEM model, access to GEM expertise, and ability to integrate with Verisk's platform for damage and loss calculations were among the primary reasons for taking this approach.

To generate losses for the two scenarios, several different model components needed to be developed. These components include:

1. An exposure model containing information about buildings in Thimphu. Building characteristics include construction materials, occupancy (building use), number of stories, year of construction, and gross area
2. A hazard/intensity model consisting of the simulated events in a model catalog. Each event in the catalog is a simulation of either the Mw7 or Mw8 scenario, with each simulated scenario described by a geographic extent (footprint) and shaking intensity.
3. A vulnerability model relating the intensity to an amount of damage. The model contains a number of different damage functions for each unique combination of construction, number of stories and year of construction.

GHI and the Thimphu Earthquake Hazard Working Group (Working Group) compiled survey data covering Thimphu to understand the building stock of the region. The results of the Thimphu Building survey ("survey") were used to develop the exposure model for this analysis.

The AIR team combined and scrubbed the Thimphu survey data in preparation for modeling. The effort included applying certain assumptions, mapping construction and occupancy descriptions in the surveys to AIR codes and importing the exposure data into the Verisk modeling platform (Touchstone). Additional details of the exposure data analysis are presented in the next section of this report.

AIR selected two scenarios for this analysis, developed in consultation with the Working Group and confirmed by GHI. The selected scenarios include a regional magnitude (Mw) 8 event on the Main Himalayan Thrust (MHT) similar to the 1714 Earthquake, and a local Mw7 event along the Dhubri-Chunthang Fault Zone (DCFZ). Localized site conditions were approximated using the United States Geological Survey (USGS) Global Slope-Based Vs30 model.

Different ground motion prediction equations (GMPEs) were selected to develop ground shaking footprints for each scenario. Two hundred possible ground shaking footprints were produced for each scenario/GMPE combination, to reflect the uncertainty of GMPE estimates.

Damage functions for unique combinations of construction, number of stories and year of construction were recommended by GEM and adopted in this study. For the risk assessment of buildings with unknown attributes, AIR developed “unknown” damage functions, as weighted averages of vulnerabilities for buildings with known attributes.

After finalization, the hazard/intensity and vulnerability components were converted into a custom model using the Model Builder tool (AIR Worldwide, 2018). Model Builder takes as input a catalog of events, associated intensities, and vulnerability functions, such as those developed here, to create a customized view of risk. The resulting model was imported into Touchstone and used to generate losses against the Thimphu exposure data.

Lastly, a series of sensitivity tests was conducted in order to fine tune the exposure, hazard/intensity and vulnerability model components and evaluate the impact of different assumptions and modelling decisions on modelled losses. The purpose of the tests was to help identify the factors that are driving model results and were used to fill in gaps of unknown values, such as in the exposure or ground motion models.

Figure 1 presents a graphical summary of the modeling methodology.

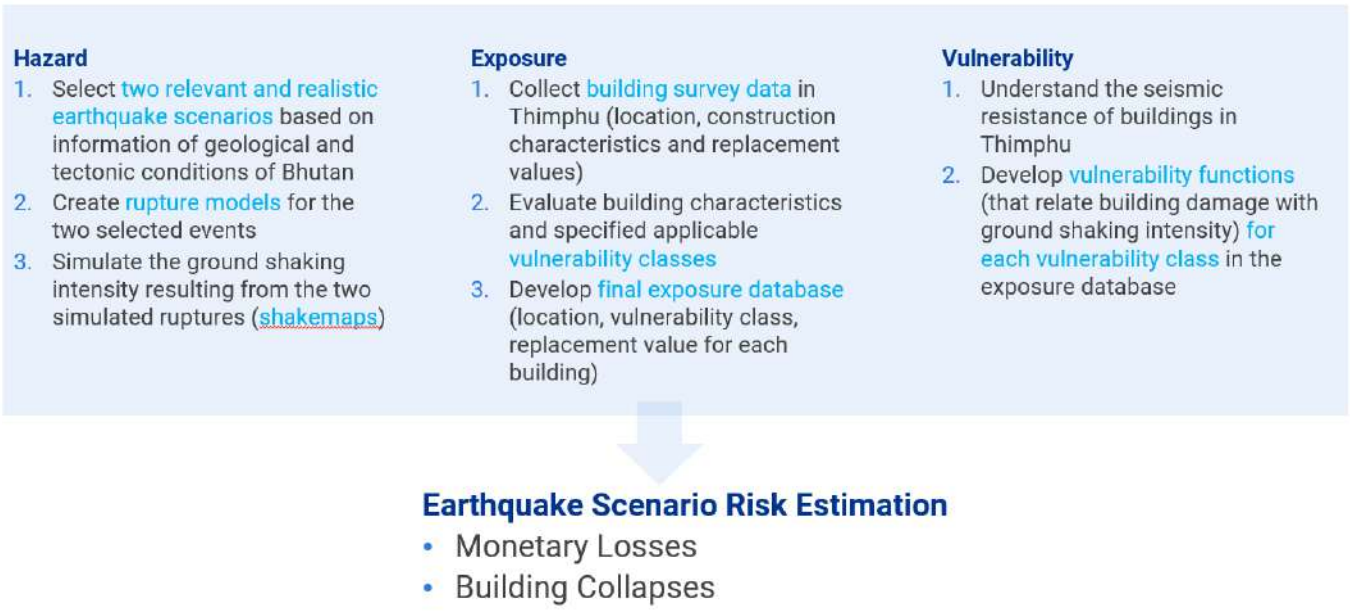

Figure 1: Schematic summary of the risk assessment methodology and results

Data and Models

The following section provides more detail on the processes followed to generate the model components necessary to produce modeled earthquake losses in Thimphu.

Exposure Model

As previously stated, GHI and the Working Group compiled survey data covering Thimphu to understand the building stock of the region. The results of the survey were used to develop the exposure model for this analysis. There were approximately 10,000 locations in the survey, but building attributes were available for approximately half the locations. The survey area is shown in figure 2 below.

Duplicate records first needed to be identified and removed before any assumptions regarding the building attributes could be made. The raw datafiles were imported into a geographic information system application (QGIS v3.14.16). A number of processing steps were taken to ensure that exposure model was as complete as possible. Duplicate records were identified and removed to avoid overestimating the risk in Thimphu. The resulting exposure model contained 9,017 unique buildings with varying degrees of completeness with regards to modellable building characteristics.

The following assumptions were made based on the subset of data for which data attributes were made available. The assumptions were developed in consultation with GHI and reviewed with the Working Group and used to convert the survey data into a format that AIR could utilize in Touchstone.

1. The survey data field titled "**Construction**" contained two distinct values, "House" and "Building". Equivalent AIR construction types were assigned prior to any loss modeling. AIR determined that "Unreinforced Masonry – Bearing Wall" and "Reinforced Concrete" were appropriate AIR construction type equivalents. These construction descriptions were used for assigning the appropriate GEM damage function.
2. Locations coded as "**House**" in the survey were assumed to be constructed with Unreinforced Masonry - Bearing Wall
3. Locations coded as "**Building**" in the survey were assumed to be constructed with Reinforced Concrete
4. Structures of the "**Building"** class constructed before 1997 were assumed not to have been seismically designed. Buildings constructed after 1997 were assumed to comply with the Indian ductile concrete code, IS 13920.
5. The survey data field titled "**Use Type**" contained several distinct values. A table containing each distinct value for "**Use Type"** from the survey and the equivalent AIR occupancy description is provided below:

Table 1: Survey to AIR mapping scheme for building uses

Use Type	AIR Occupancy Description
Commercial/Industrial Uses	General Commercial
Residential/Institutional Building Use	General Residential
Residential	General Residential
Community	Entertainment and Recreation
Institute	Universities, Colleges and Technical Schools
Commercial	General Commercial
School	Primary, Lower, Middle and Higher Secondary Schools

Use Type	AIR Occupancy Description
Industries	General Industrial
Office	Professional, Technical
Religious Building	Religion and Non-Profit

6. The data field in the survey titled "**plinthArea**" was assumed to be the building's gross area (in square meters).
7. Locations in the survey with a number of stories value of zero were assumed to be unknown.
8. Building replacement values were calculated using each location's gross area, number of stories, and construction costs. A list of construction costs was provided by the Working Group. AIR assigned a construction cost to each location based on the value in the "**Construction"** field in the survey. Several of the provided construction costs were applicable to the AIR construction type that was assigned to locations coded as "**House**" (Unreinforced Masonry – Bearing Wall). Therefore, AIR assumed that the construction cost of all locations in the survey coded as "**House**" was the median value of all the costs provided by the Client, at USD 26,404 per 75 square meters per floor. One specific construction cost in the provided list was applicable to the AIR construction type that was assigned to the locations coded as "**Building**" (Reinforced Concrete). AIR assumed that the construction cost for all locations coded as "**Building**" in the survey to be USD 33,407 per 75 square meters per floor.

    - For buildings with unknown attributes, AIR used weighted averages of gross area and/or number of stories and/or construction costs. These were based on the attributes of buildings for which all the data necessary for the calculation of the replacement value were available. Weights were computed as the percentage contribution to total number of buildings with known attributes.
    - To better represent the spatial variation of building construction and replacement value, AIR divided the building portfolio in three regions - north, central and south – and different weighted averages were computed for each region. See figure below.

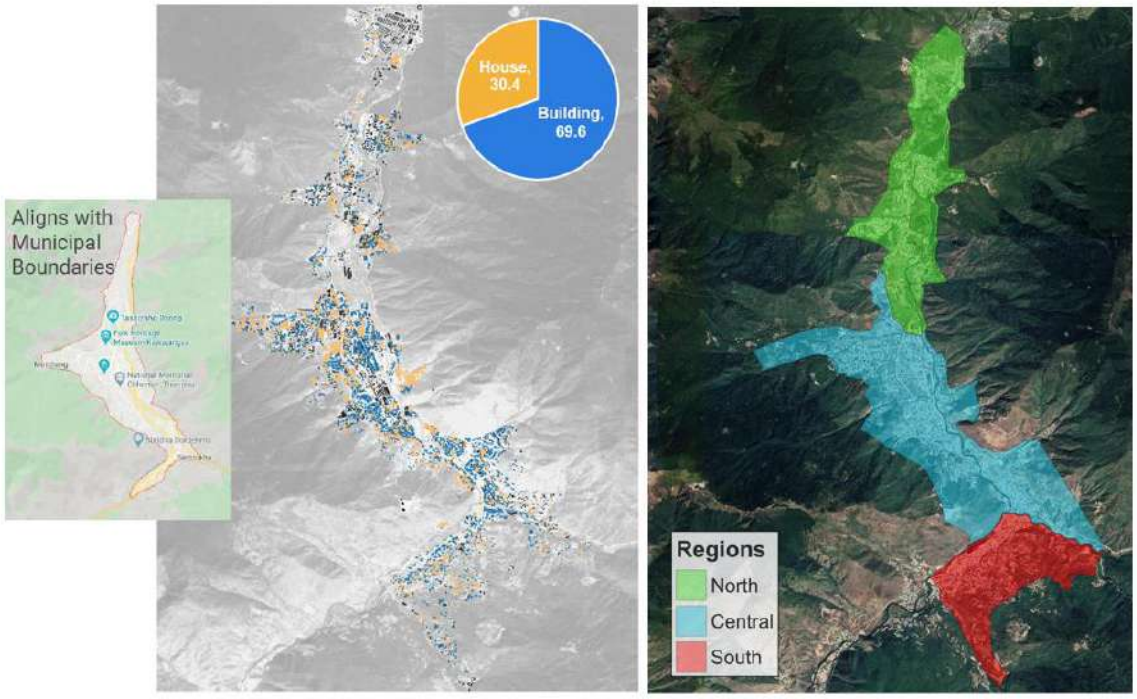

Figure 2: The survey area (left) and areas divided into three regions (North, Central and South). The 3 regions were used to inform replacement values and damage functions for locations missing key attributes.

9. The contents replacement value was calculated as a percent of the building replacement value, based on the location's line of business (LOB; Residential, Commercial or Industrial). AIR assumed that the relationship of building to contents replacement values in Thimphu was similar to that in India. AIR developed the relationship of building to contents replacement values in India during the construction of its Industry Exposure Database (AIR Worldwide, 2016a), which utilized governmental reports from agencies such as the Ministry of Home Affairs, India Central Public Work Department and India Housing Survey. The amount of contents replacement value by LOB is:

    - Residential: 25% of building replacement value
    - Commercial: Equal to building replacement value
    - Industrial: 133% of building replacement value

    Contents replacement value for locations with unknown LOB information were computed using a similar methodology used to calculate the building replacement value of structures without attributes. AIR used weighted averages

of building to contents replacement value ratios based on the attributes of locations for which the data is available. This was done for each geographic region (i.e. North, Central and South) separately.

The following figures present the percent contribution to the total number of buildings and replacement value by construction type, occupancy, year of construction (pre- and post-1997) and number of stories. Total replacement value is the sum of the costs to rebuild each structure and/or replace any contents that could be damaged in an earthquake event. The replacement values for each structure and its contents were determined as per the assumptions made above. There are 9,017 buildings in the exposure model with a total replacement value of USD 2.8bn.

Buildings with unknown construction class, occupancy type, year of construction, or number of stories are included in comparison of the percent contribution to total number of buildings, to illustrate the proportion of locations with missing attributes (denoted as "unknown" in the figures below). Only locations with known attributes were considered in the comparison of the percent contribution to Total Replacement Value shown below.

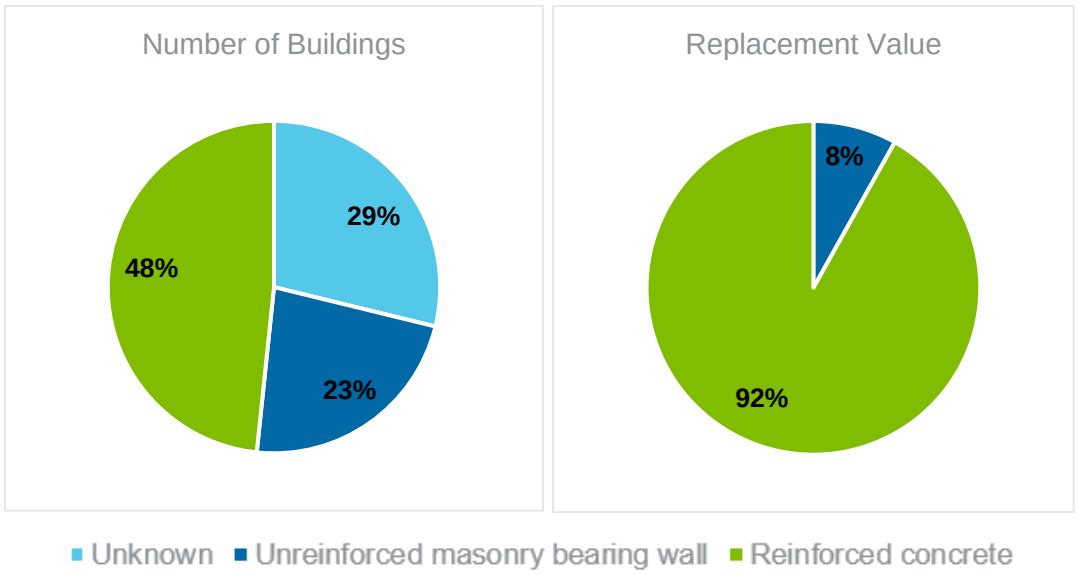

Figure 3: Percent contribution to total number of buildings and replacement value by construction type. Buildings with unknown construction types are not included in the percent contribution to total replacement value.

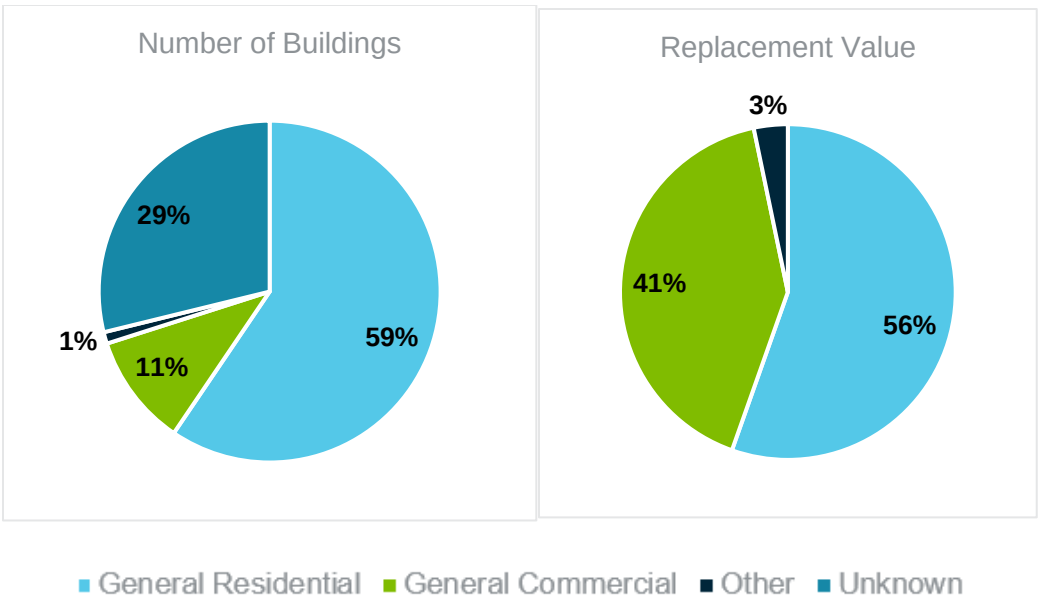

Figure 4: Percent contribution to total number of buildings and replacement value by occupancy type. Buildings with unknown occupancy type are not included in the percent contribution to total replacement value.

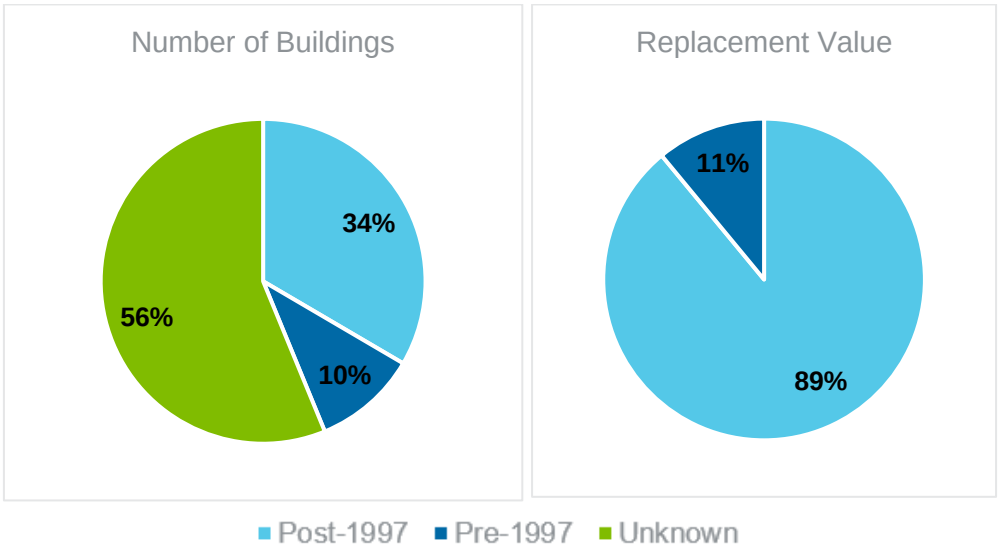

Figure 5: Percent contribution to total number of buildings and replacement value by year of construction (pre- and post-1997). Buildings with unknown year of construction are not included in the percent contribution to total replacement value.

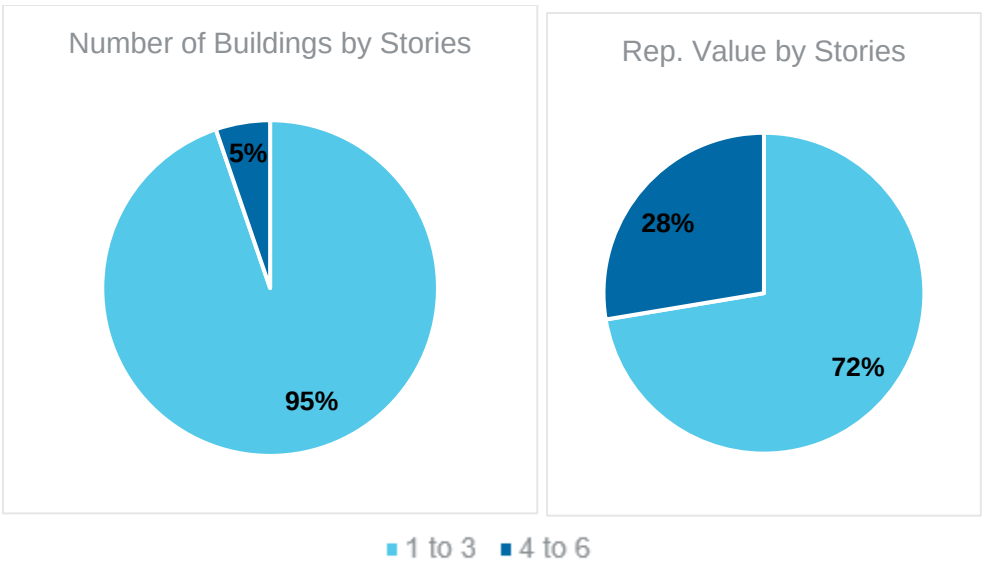

Figure 6: Percent contribution to total number of buildings and replacement value by number of stories for buildings that were constructed prior to 1997. Buildings with unknown number of stories are not included in the percent contribution to total replacement value.

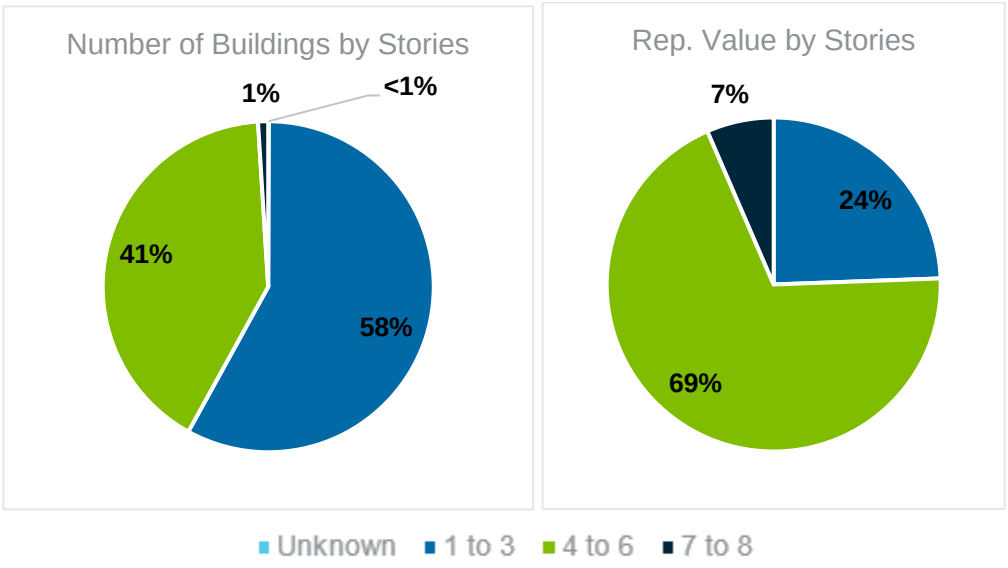

Figure 7: Percent contribution to total number of buildings and replacement value by number of stories for buildings that were constructed after 1997. Buildings with unknown number of stories are not included in the percent contribution to total replacement.

Hazard Model

Two earthquake scenarios were selected and confirmed by GHI and the Working Group to be modeled in this analysis. This section describes the details of the scenarios and the associated modeling assumptions.

Event Generation

The scenario descriptions and parameters are presented below.

- Scenario 1: A magnitude (Mw) 8 event on the Main Himalayan Thrust (MHT), similar to the 1714 earthquake
- Scenario 2: A Mw7 event along the Dhubri-Chungthang Fault Zone (DCF) at a depth below the MHT event

Table 2: Event parameters for the two selected scenarios

	Scenario 1	**Scenario 2**
Fault Name	Main Himalayan Fault	Dhubri-Chungthang dextral fault – below MHT
Fault Dip	10.0	89.0
Mw	8.0	7.0
Epicenter Longitude	90.467	88.817
Epicenter Latitude	27.362	27.368
Depth	9.985	32.0
Rake	90.0	-141
Upper Fault Depth	0.0	20.0
Lower Fault Depth	20.0	32.0

The rupture geometry for scenario 1 (see figure 8) was inferred from GEM Global Active Faults Database, as well as specific information on the MHT. The event is a single planar dip similar to the 2015 Gorkha, Nepal earthquake. The epicenter is chosen to be similar to that of the 1714 earthquake in Bhutan.

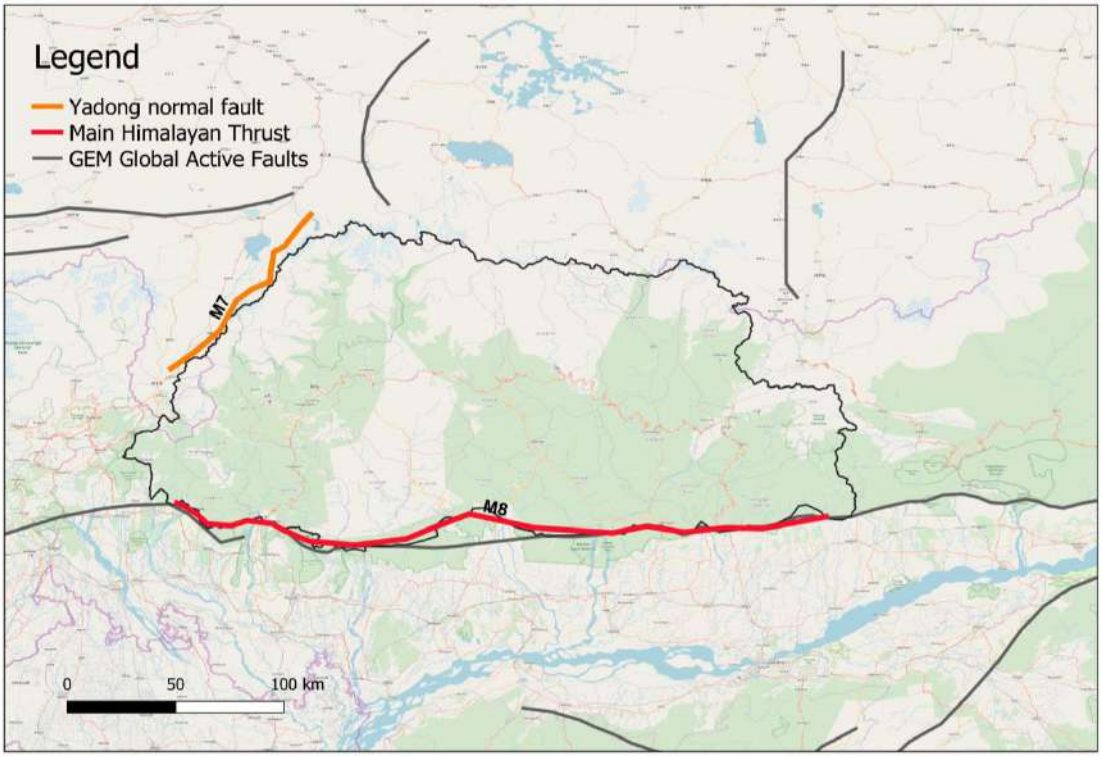

Figure 8.Faults and location surrounding scenario 1.

Scenario 2 (figure 9) is based on the 1980 Mw 6.3 event, utilizing the same epicenter, strike, dip, and rake (the rupture proceeds southeast from the epicenter). The event is modeled as located below the MHT but with a shallower depth than occurred in 1980.

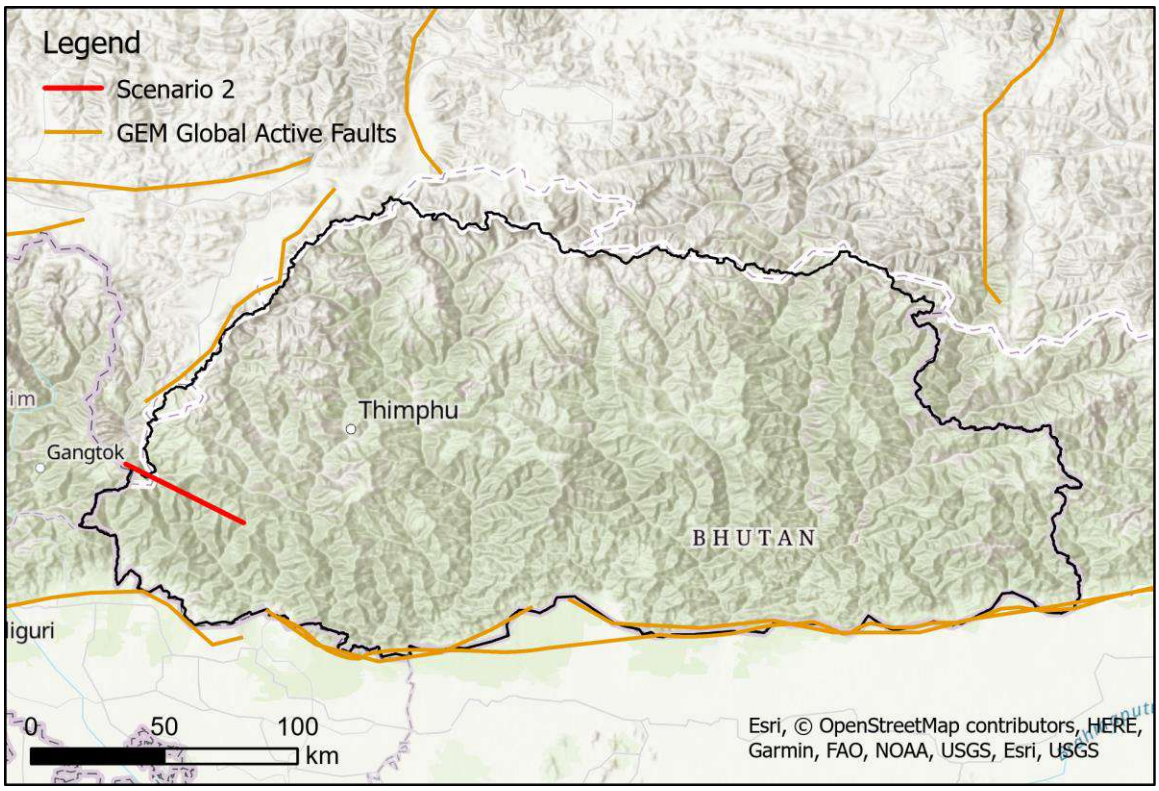

Figure 9. Location and fault descriptions for scenario 2 (thick red line) along the Dhubri-Chungtang Fault zone in southwest Bhutan.

Site Conditions

Modeling site conditions is an important aspect of earthquake risk assessment, as site characteristics can have a significant impact on the intensity of ground shaking experienced at the building location. If the arriving seismic waves are of low to moderate intensity, a site with soft shallow surface material may experience significantly higher levels of ground motion compared to that of a site of stiff rock. In the case of ground motion of high intensity, the process is more complex due to the nonlinear behavior of soil materials.

For the last few decades, the state of practice has been to infer the level of ground motion amplification with respect to base rock conditions as a function of the average shallow shear wave velocity for the top 30 meters of the earth's surface at the site of interest (Vs30).

Due to a lack of information on site characteristics in Thimphu, the USGS' Global Slope-Based Vs30 model[1] was used to approximate site conditions for this analysis; Stevens et

[1] https://earthquake.usgs.gov/data/vs30/

al. (2020) made a similar assumption, The USGS Global Slope-Based Vs30 model for Bhutan is presented in the figure below.

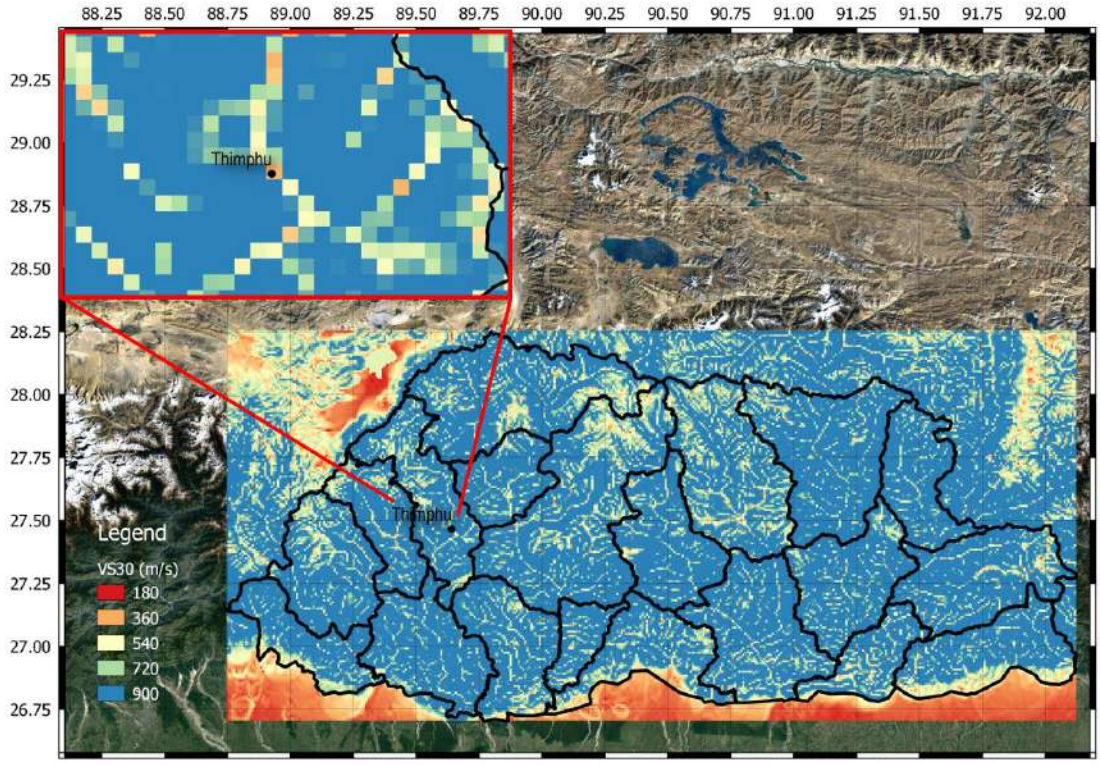

Figure 10: USGS' Global Slope-Based Vs30 model for Bhutan

Owing to the uncertainty in the soil conditions, we conducted additional sensitivity studies using Vs30 = 360m/s and Vs30 = 760m/s, encompassing a range of shear wave velocities shown in the figure above. Results are presented in more detail below.

Ground Motion Prediction Equations (GMPEs)

The selection of an appropriate ground motion prediction equation (GMPE) or combination of GMPEs for the estimation of ground shaking intensity is a key element in seismic risk assessment. In this study, different GMPEs were selected to develop ground shaking footprints for each scenario. For scenario 1, several studies use subduction interface GMPEs for events in the MHT. These equations are as follows:

- Atkinson and Boore, 2003[2]

[2] https://docs.openquake.org/oq-hazardlib/0.24/_modules/openquake/hazardlib/gsim/atkinson_boore_2003.html#AtkinsonBoore2003SInter

- Atkinson and Macias, 2009[3]
- Zhao et al., 2006[4]
- Kanno et al., 2006[5]
- Sharma et al., 2009[6]

For scenario 2, since the Yadong normal fault is located at the southern edge of the Tibetan plateau a GMPE for active shallow crust may be more appropriate. The USGS uses the following GMPEs to produce shakemaps for the 1980 Sikkim earthquake (on which scenario 2 is based):

- Abrahamason et al., 2014[7]
- Boore et al., 2014[8]
- Cambpel and Bozorgnia, 2014[9]
- Chiou and Youngs, 2014[10]

It is also worth noting that Chiou and Youngs, 2014 is recommended by GEM and was also used by USGS for the Ghorka earthquake.

Two hundred possible ground shaking footprints were produced for each scenario and GMPE combination, to reflect the uncertainty of GMPE estimates. The spatial correlation of ground shaking is explicitly accounted for in the development of each individual footprint, using the spatial correlation model by Jayaram and Baker[11], implemented in the GEM OpenQuake engine. The GMPEs of Atkinson and Macias (2009), Kanno et al. (2006) and Sharma et al (2009) do not support the functionality necessary to produce

[3] https://docs.openquake.org/oq-hazardlib/0.24/_modules/openquake/hazardlib/gsim/atkinson_macias_2009.html#AtkinsonMacias2009
[4] https://docs.openquake.org/oq-hazardlib/0.24/_modules/openquake/hazardlib/gsim/zhao_2006.html#ZhaoEtAl2006SInter
[5] https://docs.openquake.org/oq-hazardlib/0.24/_modules/openquake/hazardlib/gsim/kanno_2006.html#Kanno2006Shallow
[6] https://docs.openquake.org/oq-hazardlib/0.24/_modules/openquake/hazardlib/gsim/sharma_2009.html#SharmaEtAl2009
[7] https://docs.openquake.org/oq-hazardlib/0.21/gsim/abrahamson_2014.html
[8] https://docs.openquake.org/oq-hazardlib/0.12/gsim/boore_2014.html
[9] https://docs.openquake.org/oq-hazardlib/0.12/gsim/campbell_bozorgnia_2014.html
[10] https://docs.openquake.org/oq-hazardlib/0.24/_modules/openquake/hazardlib/gsim/chiou_youngs_2014.html#ChiouYoungs2014
[11] Jayaram, N., & Baker, J. W. (2009). Correlation model for spatially distributed ground-motion intensities. Earthquake Engineering & Structural Dynamics, 38(15), 1687–1708. doi:10.1002/eqe.922

spatially correlated ground shaking footprints. Spatial correlation of ground motion is not considered for these GMPEs.

The following figures illustrate the mean, lower and upper bound ground shaking footprints for each scenario, in terms of peak ground acceleration - PGA (in units of g). Mean, lower bound and upper bound PGA values at each location were obtained from all the ground shaking footprints produced for each scenario (200 footprints per GMPE applicable to each scenario). The lower and upper bound PGA values correspond respectively to 10 and 90- percentiles. The PGA estimates shown below are in line with findings of Stevens et al, (2020), particularly in the observation that PGA values exceeding 1.0g could be experienced in many areas were this event to recur.

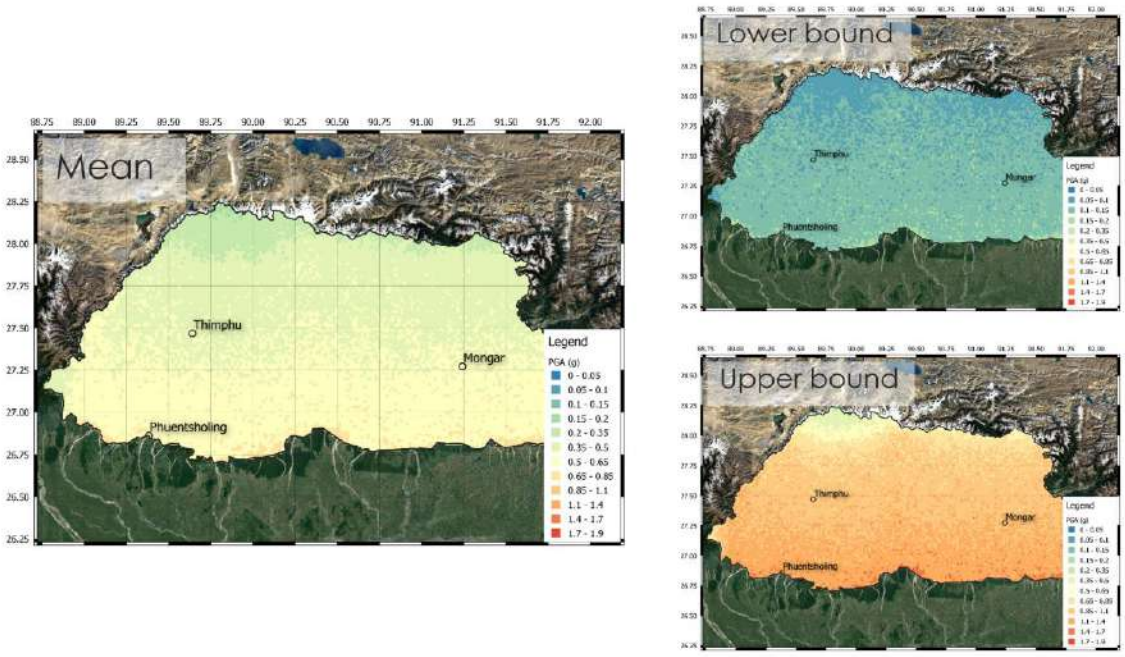

Figure 11: Mean, lower bound and upper bound ground shaking footprints (PGA, g) for Scenario 1

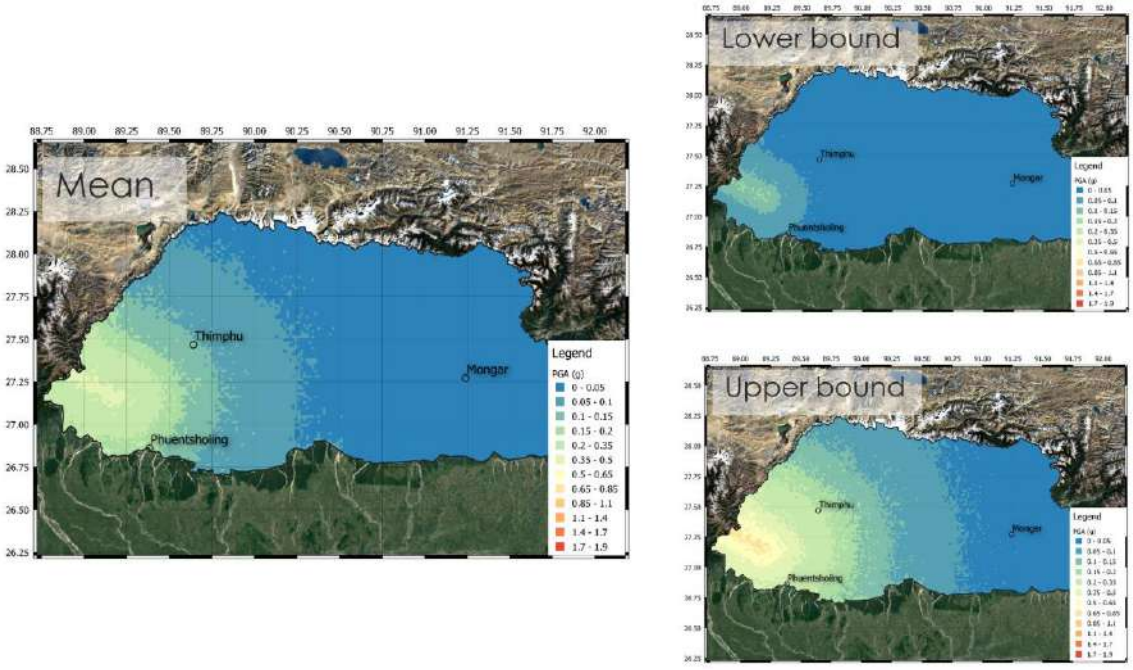

Figure 12: Mean, lower bound and upper bound ground shaking footprints (PGA, g) for Scenario 2

Vulnerability Model

Damage functions for unique combinations of construction, number of stories and year of construction outlined in the sections above were recommended by GEM and adopted in this study. A detailed discussion of the GEM fragility and vulnerability functions, along with a description of the GEM vulnerability assessment methodology is presented in the interim report (AIR, 2020).

Damage functions for buildings that were described as "**House**" (assumed to be constructed from unreinforced masonry – load bearing materials) were developed from available GEM vulnerability curves for the following building classes:

- Rubble stone masonry
- Dressed stone masonry
- Unreinforced clay brick masonry

These functions vary by number of stories, but no distinction was made with regards to year of construction.

Damage functions for locations that were described as "**Building**" varied as a function of number of stories and year of construction. Buildings constructed prior to 1997 were assigned non-ductile reinforced concrete functions made available by GEM and were

assumed to have no soft stories. Buildings constructed after 1997 were assumed to comply with the Indian ductile concrete code, IS 13920. This code establishes provisions for ductile detailing of reinforced concrete structures subjected to seismic action. However, the corresponding criteria for earthquake analysis and design are based on the Indian Standard IS 1893 (from 1984).

The IS 1893 provisions follow a simplified modal analysis and response spectrum-based approach for the definition of seismic demand, which is not as sophisticated as modern design regulations based on capacity design and performance-based assessment. As a result, we assumed that reinforced concrete buildings constructed after 1997 have moderate ductility (instead of high ductility, which is expected in buildings designed and constructed following more modern buildings codes).

For the risk assessment of buildings with unknown attributes, AIR developed “unknown” damage functions, as weighted averages of vulnerabilities for buildings with known attributes. To better represent the spatial variation of building construction and vulnerability, AIR divided the building portfolio in three regions - north, central and south (see figure 2 above) and different “unknown” functions were developed for each region. In this approach, the weights for each region represented the contribution of each known building class to the total replacement value in that region. As a simplified example, if 30% of the replacement value in a region corresponds to “house” and 70% to “building”, the corresponding “unknown” function to be applied to buildings with unknown attributes in that region was a combination of “house” and “building” function, with 30% and 70% weights, respectively.

Figure 13 summarizes the vulnerability functions used in the analyses.

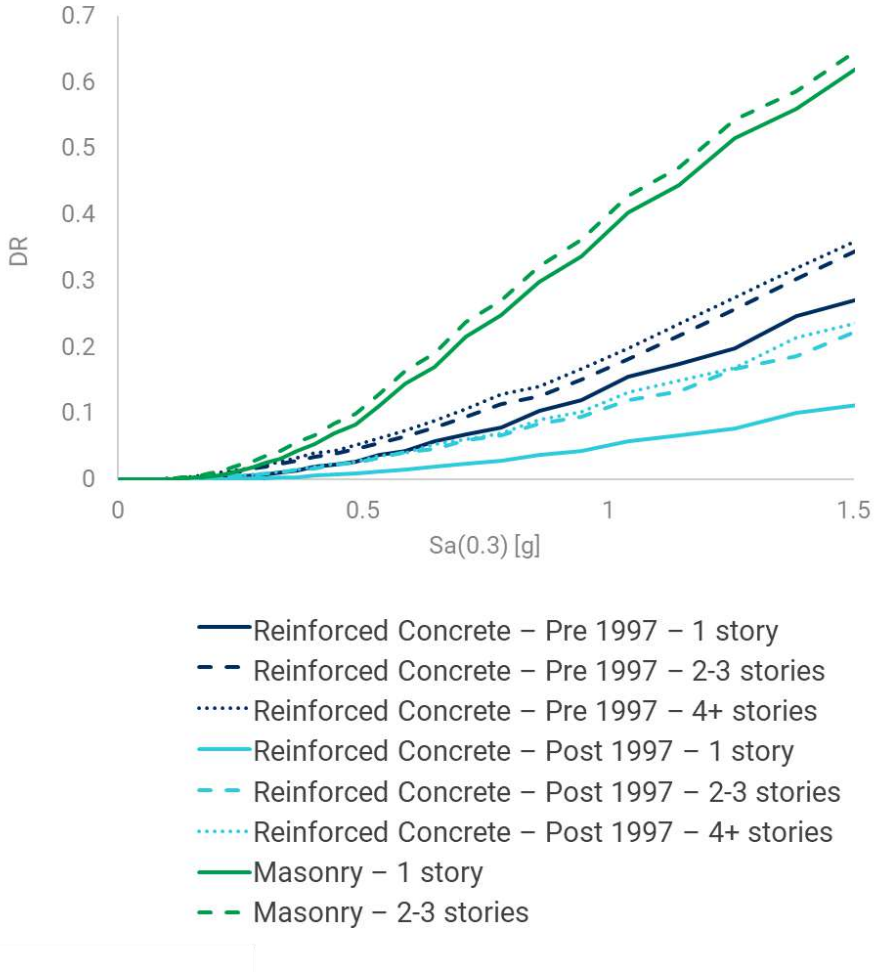

Figure 13: Summary of vulnerability functions used for loss estimation, relating spectral acceleration (Sa) to modeled damage ratio (DR).

To calculate damage and loss, AIR assembled the hazard permutations into *catalog* and associated *intensity* files. These files were then combined with a *vulnerability* file through the AIR Model Builder tool (AIR Worldwide, 2018) and implemented in AIR's Touchstone risk modeling platform. The Touchstone platform allows the hazard and vulnerability models developed for this project to be simulated against the Thimphu exposure data, utilizing the AIR software framework, financial model, and reporting capabilities.

The results are provided in the following section.

Results

The following section presents the results of the baseline study (prior to any sensitivity analysis), validation and loss benchmarking efforts. The modeled loss results are presented by scenario (Mw8 and Mw7) and GMPE.

The hazard permutations detailed above are summarized in figure 14. For scenario 1 (Mw 8, MHT) we have 5 GMPEs * 200 simulations per GMPE * 3 soil types, for a total of 3000 modeled events. For scenario 2 (Mw 7, DCF) we have , while for event 2 we have 4 GMPEs * 200 simulations per GMPE * 3 soil types, for a total of 2400 modeled events.

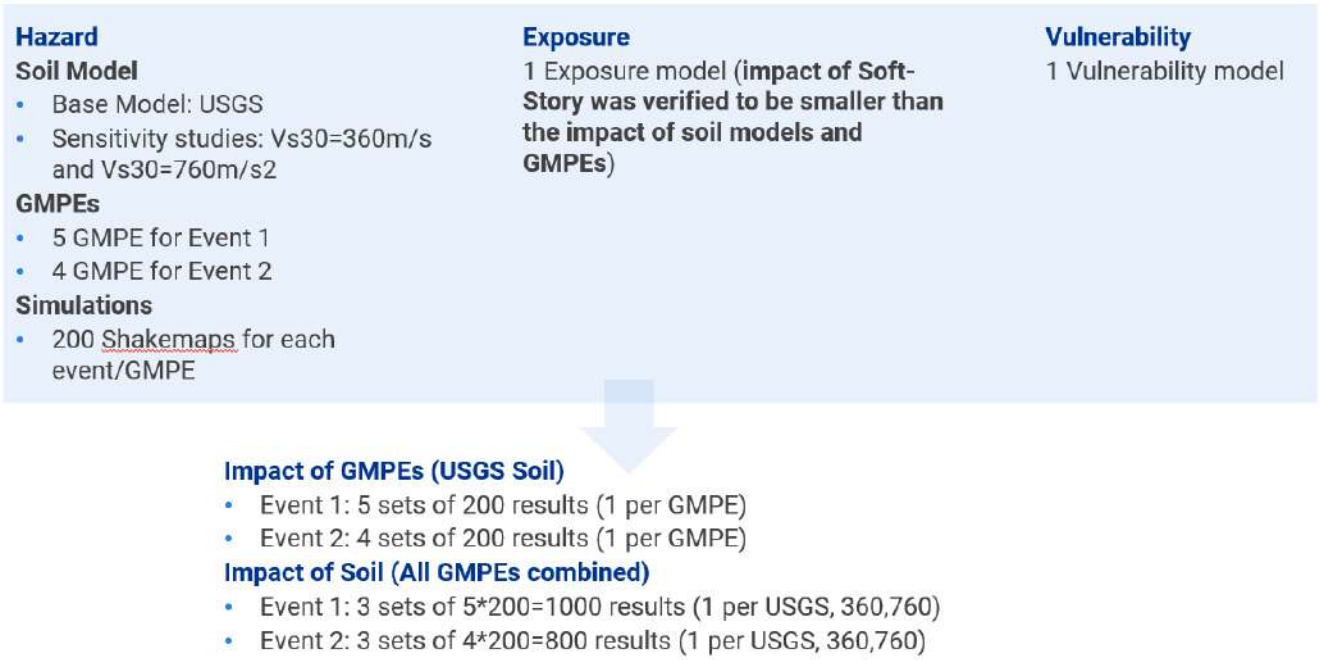

Figure 14: Summary results developed by permutations of scenario, GMPE (and associated uncertainty) and soil type. The same exposure set and vulnerability functions were used for each hazard permutation.

Summary Loss Results

Results for scenarios 1 and 2 are shown in figures 15 and 16, which consider the base USGS soil model. In each case, results are shown separately by GMPE for the mean, 10th percentile and 90th percentile losses from the 200 simulated events in order to capture the variability and impact of model assumptions.

As expected, the losses from scenario 1 are much larger, ranging from $52-$573M with a mean of $413M. Losses from scenario 2 ranging from $1-$136M with a mean of $47M.

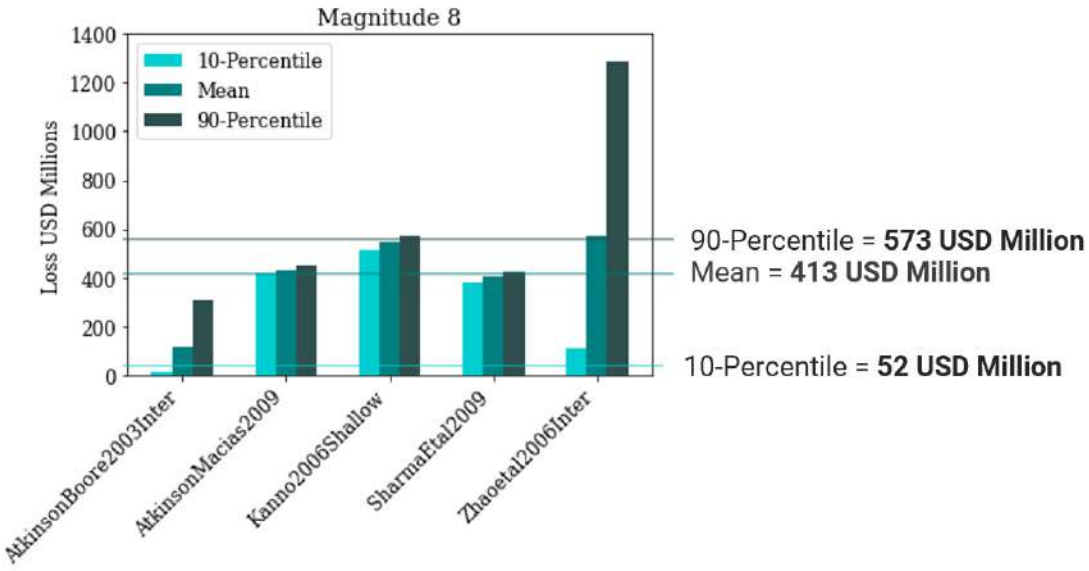

Figure 15: Modeled results for scenario 1, across different GMPEs, using the base USGS site conditions. The mean and percentiles are derived from results of 200 simulations.

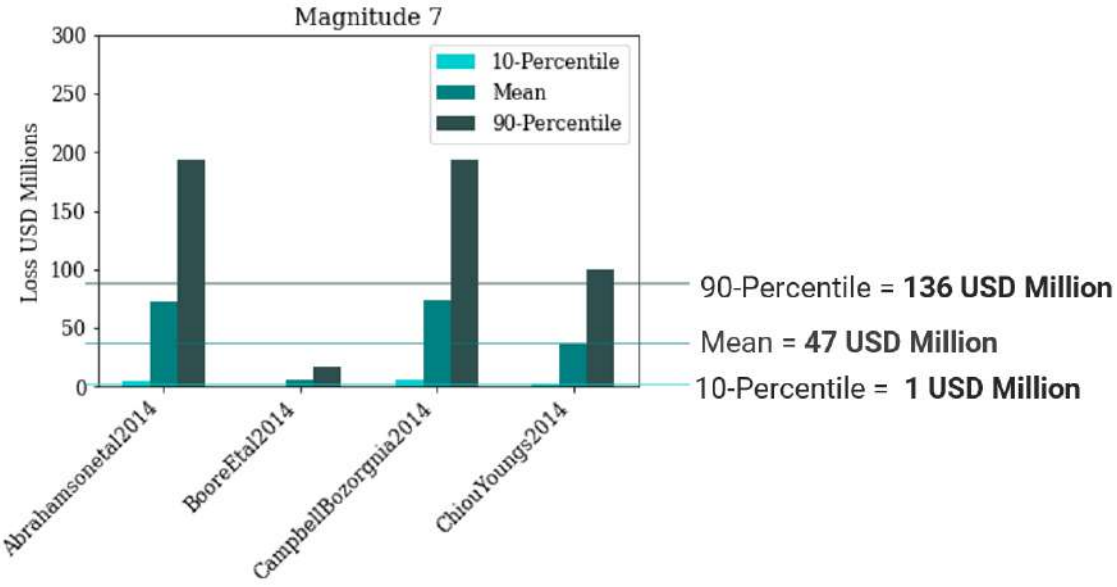

Figure 16: Modeled results for scenario 2, across different GMPEs, using the base USGS site conditions. The mean and percentiles are derived from results of 200 simulations.

Figure 17 considers sensitivity to the choice of the USGS Base Mode and shear wave velocities of Vs30 = 360m/s and Vs30 = 760m/s to characterize the site conditions. Results are computed across all 5 GMPEs (1000 simulations) for scenario 1. The line shows the mean estimate from figure 15 for comparison.

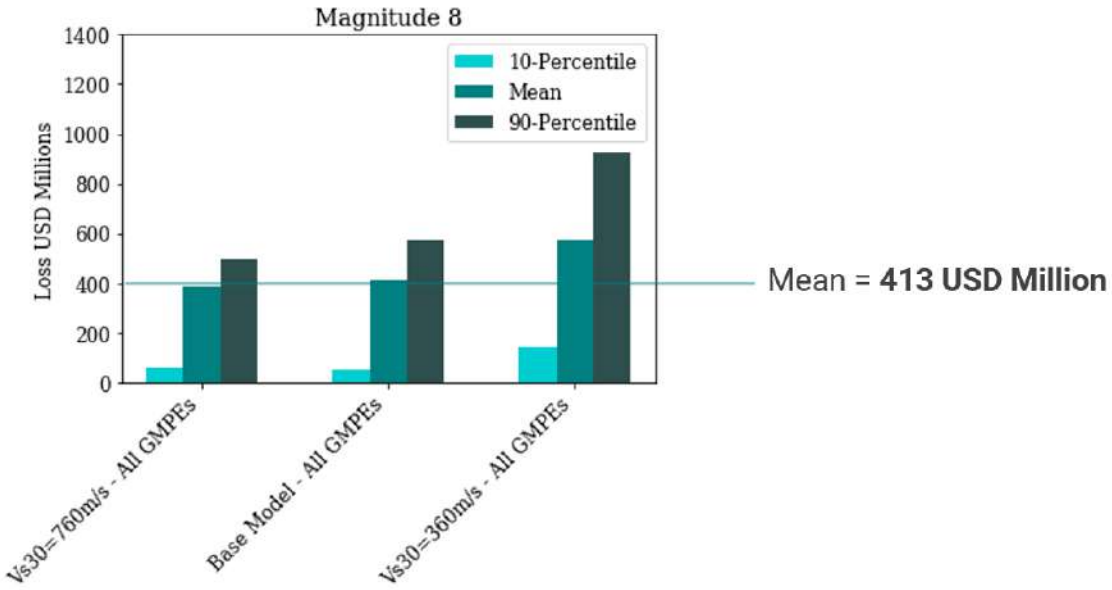

Figure 17: Sensitivity to site conditions for scenario 1, using all GMPEs.

Summary Sensitivity Results

The results in figures 15 and 16 each show good agreement across most of the GMPEs considered with one GMPE presenting as an outlier. For scenario 1, the Atkinson and Boore, 2003 results are well below the others, while for scenario 2, Boore, et al. 2004 stands out. The outliers suggest a lower confidence in the lowest modeled losses for these scenarios with moderate sensitivity in results to the other choices.

Figure 17 indicates that modeled losses are not sensitive to the site conditions, suggesting that the base USGS model is a reasonable approach to characterizing the soil response. The results for scenario 2 show a similar pattern and are not presented.

Spatial Distribution of Loss – Scenario event 1

Figure 18 provides additional detail of the spatial distribution of loss for scenario event 1. The three-panel presentation shows a heat map of absolute loss on the left, a scatter plot of the building inventory in Thimphu in the center, and a map of a simulated loss ratio for the event on the right. The loss ratio is the loss for the median simulated event divided by the building value.

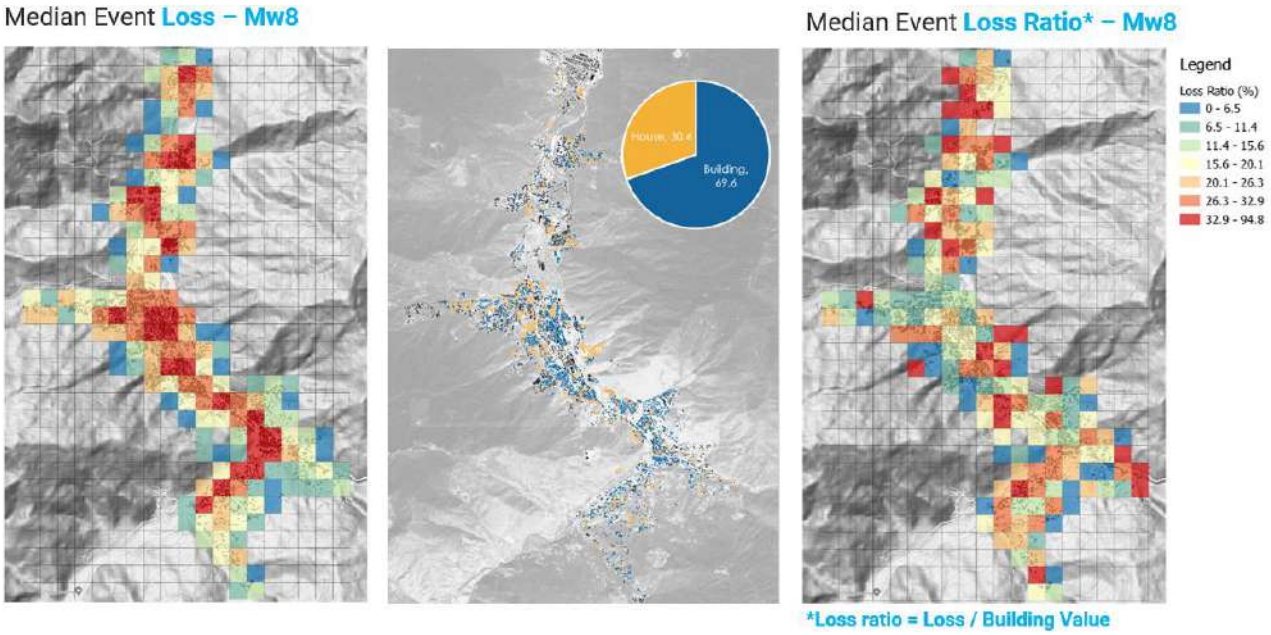

Figure 18: Spatial distribution of losses for scenario 1. Left: heat map of absolute loss; Center: scatter plot of the building inventory; Right: loss ratio for the median simulated event

The heat map of absolute loss aligns with the peak densities shown in the scatter plot; this is expected as the absolute loss is driven by not only the hazard and vulnerability but also by the exposure on the ground. However, it is worth noting that the results on the right (which are normalized by exposure) suggest that despite a higher density of exposure, buildings close to the center of the city are less vulnerable (likely due to the higher proportion of superior construction of buildings in this area) than those on the outer edge of the capital. The grids in red highlight the most vulnerable areas.

The losses for scenario 2 are significantly lower and are not shown.

Collapse Probabilities

The final set of scenario results are presented in figure 19 (again for scenario 1 only). The two panels show the estimated distribution of building collapse for reinforced concrete (left) and masonry (right) estimated from the GEM fragility functions. The plots clearly show a much higher susceptibility of collapse amongst the masonry buildings; of the 400 estimated building collapses with this scenario, 3 in 4 are expected to occur in the unreinforced masonry buildings located across the capital city (see additional commentary on collapse estimates in the validation section below).

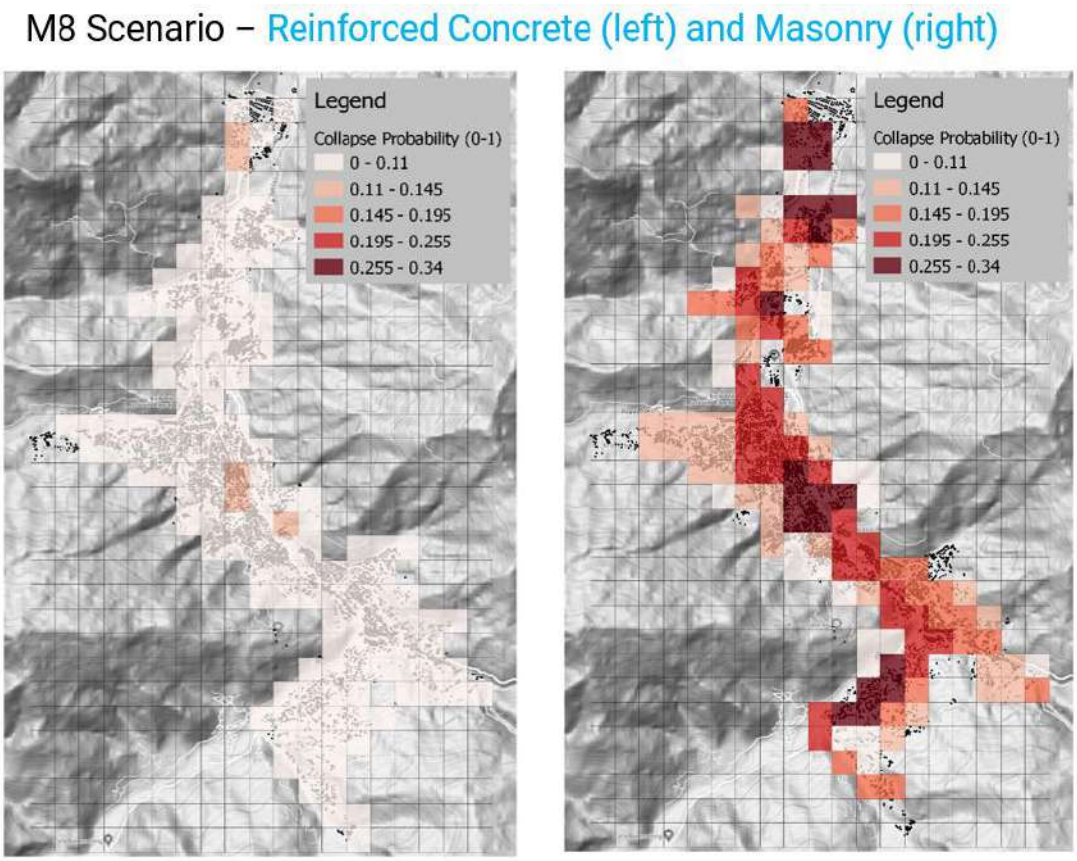

Figure 19: Estimated building collapses for scenario 1 from reinforced concrete (left) and masonry (right) construction types.

Model Benchmark – Scenario Losses for India

As a point of comparison for the scenario results presented above, AIR created comparisons of the loss ratios for exposures in India, using selection of events from the Verisk Earthquake Model for India. The comparison assumes that building standards and construction practices are similar to those in Bhutan (and Thimphu specifically), and provides a sense of how similar size events in the Verisk model compare to the scenarios from the GEM model presented here.

Table 3 shows the selection of events used for the comparison.

Year	Earthquake	Magnitude	Year	Earthquake	Magnitude
1762	Chittagong	8.8	1956	Khurja-Bulandshahr	6.7
1803	Gharwal	7.4	1960	Gurgaon	5.6
1819	Rann of Kachchh	7.7	1966	Moradabad	5.6
1864	Kathiawar	5.7	1967	Koyna	6.6
1869	Cachar-Manipur	7.3	1969	Godavari	5.7
1885	Kashmir	6.3	1975	Kinnaur	6.8
1897	Shillong	8.0	1986	Dharmsala	5.5
1900	Coimbatore-Nilgiri	6.0	1988	Bihar-Nepal	6.8
1905	Kangra	7.9	1991	Uttarkashi	6.8
1909	Kachhi	7.2	1993	Latur/Killari	6.2
1916	Dharchula	7.0	1997	Jabalpur	5.8
1918	Srimangal	7.2	1999	Chamoli	6.5
1934	Bihar-Nepal	8.0	2001	Bhuj	7.6
1936	Bihar	5.82	2005	Kashmir	7.6
1945	Chamba	6.5	2011	Sikkim	6.9
1950	Assam	8.6	2013	Bhadarwa-Kashmir	5.6
1956	Anjar	6.0	2015	Nepal	7.8

Table 3: Selected historical events from the Verisk Model for India ((AIR Worldwide, 2016b).

The comparison across the 34 historical events in India were based on the estimated "as-if" losses – expected losses if these events were to recur on today's exposure. The results are presented in figure 20 (comparison to Thimphu scenario 1) and figure 21 (comparison to Thimphu scenario 2). In each plot, we consider the variation in the loss ratio (loss divided by the building values) on the vertical axis with distance to the epicenter on the horizontal axis. The grey dots are the exposure locations in India from the Verisk model, while the red and blue dots represent the location of Thimphu from scenario 1 and scenario 2, respectively.

Figure 20 shows the comparison for scenario 1. For the Verisk model, we grouped all of the events in Table 3 with magnitudes above Mw 7 and present the average loss ratio. The 5 red dots represent the results for each of the 5 GMPEs (see figure 15 above). The result show reasonably good agreement; the loss ratios variation from 5-20% across GMPEs is similar to the range of loss ratios from the Verisk India model for locations between approximately 50 and 100km from the event epicenter.

Figure 21 shows the comparison for scenario 2; in this case we average the loss ratio from all events from the Verisk model with magnitudes between Mw 6.0 and 7.5. At first glance the results from the GEM model in blue appear to differ somewhat from the Verisk model; however, noting the scale of the vertical axis shows that the difference is on the order of 1-2%, within the uncertainty of model results. The Verisk and GEM

models both estimate low damage ratios (1-3%) at locations within 50-100km of events in this range of magnitudes.

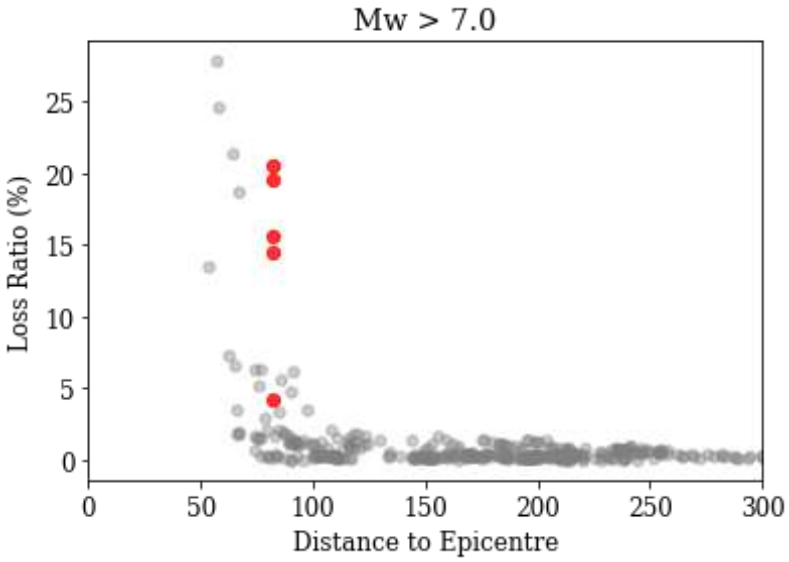

Figure 20: Loss ratios for Thimphu Scenario 1 (red dots) vs. results from Verisk Model for India at distance from epicenter (distance in km).

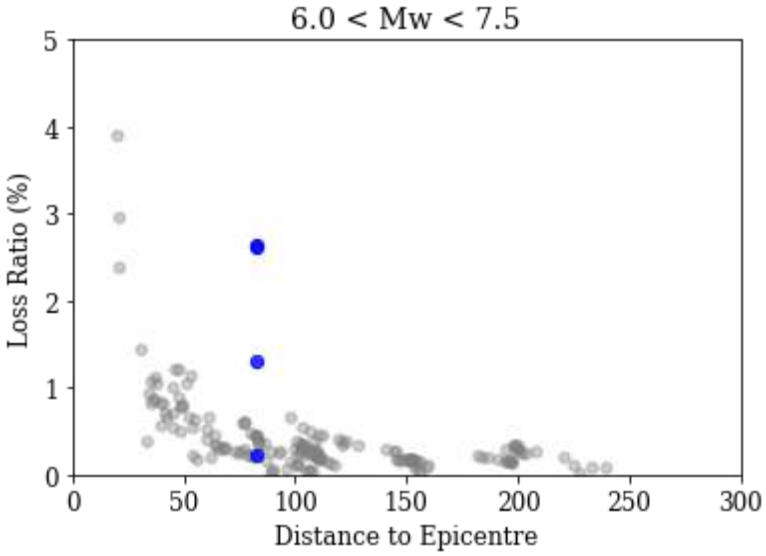

Figure 21: Loss ratios for Thimphu Scenario 2 (blue dots) vs. results from Verisk Model for India at distance from epicenter (distance in km).

A second comparison was performed to assess the relative vulnerability of the masonry and reinforced concrete building types in the Thimphu scenario model to those in the Verisk India model for the similar size events.

The relative vulnerability by class and number of stories were used as comparative metrics. Relative vulnerability is defined as the loss normalized by replacement value for all buildings, by class. Class is defined as the unique construction, occupancy, year of construction and number of stories for each modeled location. Each class has a unique damage function.

Figure 22 shows the comparison for scenario 1, using events in the Verisk India model of Mw8 and above. The vertical axis is the relative vulnerability normalized against the masonry construction (such that masonry appears as 100%), and the different colors represent the range of GMPEs considered in each model. Results for the Thimphu model are shown at left, with the Verisk model at right.

The construction types are listed across the bottom axis, with masonry types at the left in both plots and different reinforced concrete types occupying the remaining positions. While some variability exists, the main takeaway is that the various reinforced concrete types in the Thimphu and Verisk India models are significantly less vulnerable than the masonry types (RC types 20-50% as vulnerable overall).

A comparison for Thimphu scenario 2 and Verisk India model events between Mw6 and Mw7.3 (not shown) shows a similar result, with the reinforced concrete types 10-20% as vulnerable as the masonry counterparts.

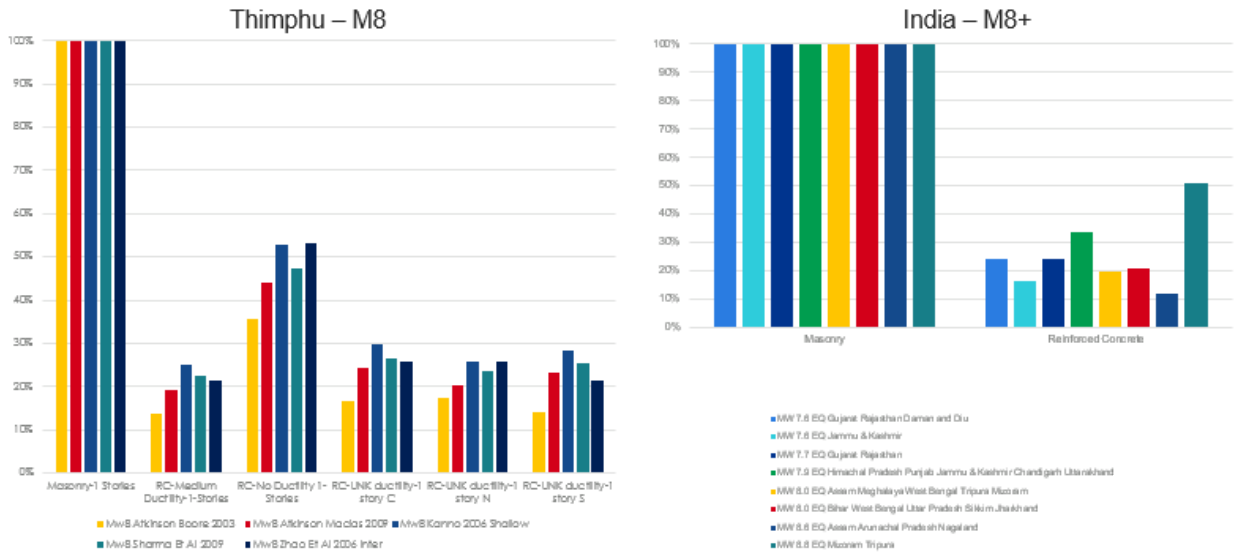

Figure 22: Relative vulnerability of masonry and reinforced concrete types in the Thimphu (left) and Verisk India (right) models.

Comparison of Collapse Estimates

A final point of comparison concerns the collapse estimates for the two scenarios. For scenario 1 (Mw8), the expected number of collapses is 400, with approximately 100 from reinforced concrete and 300 from masonry types. The estimate is further divided as approximately 8% from commercial structures and 92% from residential structures. For scenario 2 (Mw7), the mean estimate is only 10 building collapses. As described in more detail below, these estimates are lower than other collapse figures cited in studies of events in Bhutan.

Two studies are used for comparison. The first describes results of a post disaster survey following the Mw6.9 Sikkim earthquake which occurred 18 September 2011 (Joint Rapid Needs Assessment Team, 2011). The event epicenter was located near Taplejung, Nepal, and affected parts of India, Nepal, Bhutan and surrounding countries. The post disaster survey was conducted by a team from the Royal Government of Bhutan, the United Nations, and World Bank/GFDRR. Despite shaking characterized as "light" to "very light" in the affected areas, the survey noted 345 houses were completely destroyed, with another 1,660 suffering major damage and another 6,000 with minor damage. This compares to approximately 10 collapsed buildings estimated in scenario 2, which produced a similar order of magnitude shaking (0.1%g or below) in and around the 10,000 buildings in Thimphu.

While the estimates of the monetary damage to buildings in this study (mean approximately $50M) seem plausible compared to the estimate from the Sikkim event ($16M in 2011, for a similar number of affected buildings), the collapse estimate in the present study is much lower. Possible explanations for the disparity in collapse estimates include 1) a lower quality of construction (with a prevalence of rubble stone, rammed earth and other weaker types) in the mostly rural areas affected by the Sikkim earthquake, compared to the building stock in Thimphu; 2) a lack of understanding amongst survey engineers about the possibility of repairing stone masonry and rammed earth houses, which may have contributed to structures assigned to total/near collapse category; and a related issue 3) buildings with partial collapse being characterized as total collapses. In contrast the AIR estimates, where collapse was identified as 90% or greater damage ratio, the major damage threshold in the Sikkim survey assumed a 30% damage ratio. While the differences in methodology likely contribute, the discrepancy is worth noting – the low number of expected number of collapses for scenario 2 in this study may well be a very best case, and may underestimate the likelihood of severe damage and partial collapse.

A second study by Stevens, et al. (2020) on the seismic risk and hazard in Bhutan included a simulation of the 1714 Mw8 earthquake, offering a more direct comparison with scenario 1 in the present work. Figure 11 in Stevens, et al. (2020) presents exceedance probabilities for building collapses for different damage models, where each damage model includes different vulnerability curves and exposure distributions.

According to these exceedance probabilities, our estimate of 400 collapsed buildings for scenario 1 appears again to be best case outcome; the curves in their figure 11 suggest at least a 10% chance of 2000 or greater collapsed buildings. It should be noted that the authors (Stevens et al.) highlight the various uncertainties in their estimate, including the dependence on the composite vulnerability-exposure damageability model, sensitivity of results to GMPEs, and other factors. A detailed comparison to the present work is beyond the scope of this study, but the results of this comparison and the comparison with the Sikkim event survey suggest that estimates of building collapse may be highly variable and subject to significant uncertainty.

Conclusions

This work describes the implementation of an existing earthquake model developed by the Global Earthquake Model Foundation (GEM) in the Verisk modeling platform and application to a locally developed building inventory. The study focused on building losses and collapse probabilities from two earthquake scenarios: a regional magnitude (Mw) 8 event on the Main Himalayan Thrust (MHT) similar to the 1714 Earthquake, and a local Mw7 event along the Dhubri-Chunthang Fault Zone (DCFZ). The main conclusions are as follows:

- The GEM model hazard and vulnerability were successfully implemented in the Verisk modeling platform, demonstrating the utility of the study approach.
- The results for the modeled scenario were sensitive to the choice of ground motion prediction equations (GMPEs).
- Losses for the Mw8 scenario were significantly higher than the Mw7 scenario, with a best estimate of $400 million ($600m upper bound) for scenario 1 and a best estimate of $50 million ($150m upper bound) for scenario 2.
- Modeled losses and collapse probabilities for masonry buildings far exceed those estimated for reinforced concrete buildings
- Modeled damage ratios for the two scenarios and the relative vulnerability by construction class align with estimates developed from the Verisk model for India, providing a reasonable benchmark for the GEM model implementation
- Comparisons of modeled collapse estimates from this study with field observations and other seismic risk studies suggest that the estimated collapses could be underestimated. Collapse probabilities are subject to significant uncertainty and results from this study should not be used as the sole basis for building codes, disaster management or event response planning.

Additional References

AIR Worldwide, 2016a. *Industry Exposure Database for India*. AIR Model Documentation

AIR Worldwide, 2016b. *AIR Earthquake Model for India*. AIR Model Documentation

AIR Worldwide, 2018. *Developing Views of Risk with Model Builder*. AIR Solutions Brief

AIR Worldwide, 2020. *Earthquake Model for Bhutan: Overview of relevant Hazard, Exposure and Vulnerability Data*, interim report developed for GHI

Hetényi, G., R. Le Roux-Mallouf, T. Berthet, R. Cattin, C. Cauzzi, K. Phuntsho and R. Grolimund, 2016. *Joint approach combining damage and paleoseismology observations constrains the 1714A.D. Bhutan earthquake at magnitude 8±0.5.* Geophys. Res. Lett., 43, 10,695–10,702. doi:10.1002/2016GL071033.

Joint Rapid Needs Assessment Team, 2011. *September 18, 2011 Earthquake Joint Rapid Assessment for Recovery, Reconstruction and Risk Reduction*. Joint publication of the Royal Government of Bhutan, the United Nations, and World Bank/GFDRR

Royal Government of Bhutan (undated report, post 2015), *Bhutan Disaster Risk Management Status Review*, Department of Disaster Management. ISBN 978-99936-949-1-5

Stevens, V.L., R. De Risi, R. Le Roux-Mallouf, D. Drukpa and G. Hetényi, 2020. *Seismic Hazard and Risk in Bhutan*. Natural Hazards, 104, 2339–2367. doi:10.1007/s11069-020-04275-3

Wangchuk, T. 2017. *Country Report for Bhutan*. Asian Disaster Reduction Center

World Bank Group, undated report. *Seismic Risk Assessment in Thimpu Bhutan*. Global Facility for Disaster Reduction and Recovery.

About Verisk Extreme Event Solutions

Verisk provides risk modeling solutions that make individuals, businesses, and society more resilient to extreme events. In 1987, Extreme Event Solutions (formerly AIR Worldwide), a Verisk subsidiary, founded the catastrophe modeling industry and today models the risk from natural catastrophes, terrorism, pandemics, casualty catastrophes, and cyber incidents. Insurance, reinsurance, financial, corporate, and government clients rely on Verisk's advanced science, software, and consulting services for catastrophe risk management, insurance-linked securities, longevity modeling, site-specific engineering analyses, and agricultural risk management. Verisk is headquartered in Jersey City, New Jersey with many offices throughout the United States and around the world.

For more information about Verisk, a leading data analytics provider serving customers in insurance, energy and specialized markets, and financial services, please visit www.verisk.com

For more information on our Boston headquarters and additional offices in North America, Europe, and Asia, visit www.air-worldwide.com/About-AIR/Offices/